High-Efficiency Bidirectional DAB Inverter Using a Novel Hybrid Modulation for Stand-Alone Power Generating System With Low Input Voltage

Yong-Won Cho, Woo-Jun Cha, Jung-Min Kwon, *Member, IEEE*, and Bong-Hwan Kwon, *Member, IEEE*

***Abstract*—This paper proposes a high-efficiency bidirectional dual-active-bridge (DAB) inverter using a novel hybrid modulation for a stand-alone power generating system with a low input voltage. The proposed DAB inverter consists of a DAB dc–dc converter and a synchronous rectifier (SR) for unfolding. The DAB dc–dc converter transforms the low dc voltage into a rectified sine wave that pulsates twice the grid frequency. The rectified sine wave unfolds into the grid voltage by SR. The proposed hybrid modulation combines a phase shift control and a variable frequency control. The variable frequency control converts the nonlinear function of the phase shift angle into a linear function and controls the output power. This leads to a simple closed-loop control for the sinusoidal current waveform, a low harmonic distortion, and a high-voltage conversion ratio without an increase of the transformer turn ratio. Since the proposed DAB inverter has only a single power conversion stage, it has a simple structure, high power density, and low cost. It also has a high efficiency of 94.2% by a zero-voltage switching (ZVS) turn on of the switches in two full bridges (FBs). The operation principle of the proposed DAB inverter using this hybrid modulation is analyzed and verified. Experimental results for a 1-kW prototype are obtained to show the performance.**

***Index Terms*—Dual-active-bridge (DAB) inverter, hybrid modulation, single power conversion.**

I. Introduction

GENERALLY, stand-alone generating systems require high efficiency, high reliability, small size, and low cost. For household electric supply, the cost and size are important elements. As an uninterrupted power supply (UPS) used in internet data centers, hospitals, and militaries, it is also important to provide reliable and high-quality power since a power failure can cause serious problems such as data loss, injuries, fatalities, or business disruption [1]. The off-line UPS is now the most commonly used technology for supplying power to critical loads such as computers and medical equipment. When utility power is not available, it provides regulated emergency power to the connected equipment by supplying power from a separate source.

In the off-line UPS system, the load is directly connected to ac power source, typically the grid, or ac loads. When the grid fails or goes below a minimum level, the off-line UPS blocks the incoming grid power and delivers power to the ac load via a dc–ac inverter system with an internal storage battery. The

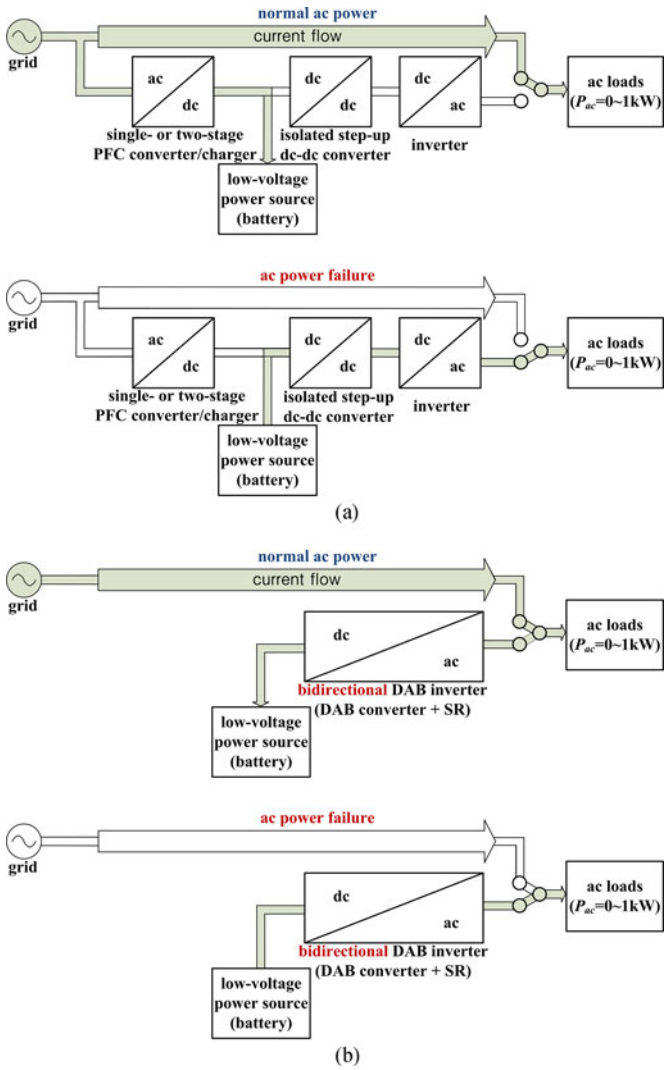

Fig. 1. Block diagrams of the stand-alone power generating system for off-line UPSs. (a) The conventional stand-alone generating system with three or four power conversion stages. (b) The proposed stand-alone generating system with single power conversion stage.

Manuscript received April 15, 2015; revised June 14, 2015 and August 16, 2015; accepted August 20, 2015. Date of publication September 3, 2015; date of current version January 7, 2016. Recommended for publication by Associate Editor Prof. J. Itoh.

Y.-W. Cho and W.-J. Cha are with the Department of Electrical Engineering, Pohang University of Science and Technology, Pohang 790-784, Korea (e-mail: ywcho@postech.ac.kr; woojun79@postech.ac.kr).

J.-M. Kwon is with the Department of Electrical Engineering, Hanbat National University, Daejeon 305-719, Korea (e-mail: jmkwon@hanbat.ac.kr).

B.-H. Kwon is with the Department of Electronic and Electrical Engineering, Pohang University of Science and Technology (POSTECH), Pohang 790-784, Korea (e-mail: jmkwon@hanbat.ac.kr).

Color versions of one or more of the figures in this paper are available online at http://ieeexplore.ieee.org.

Digital Object Identifier 10.1109/TPEL.2015.2476336

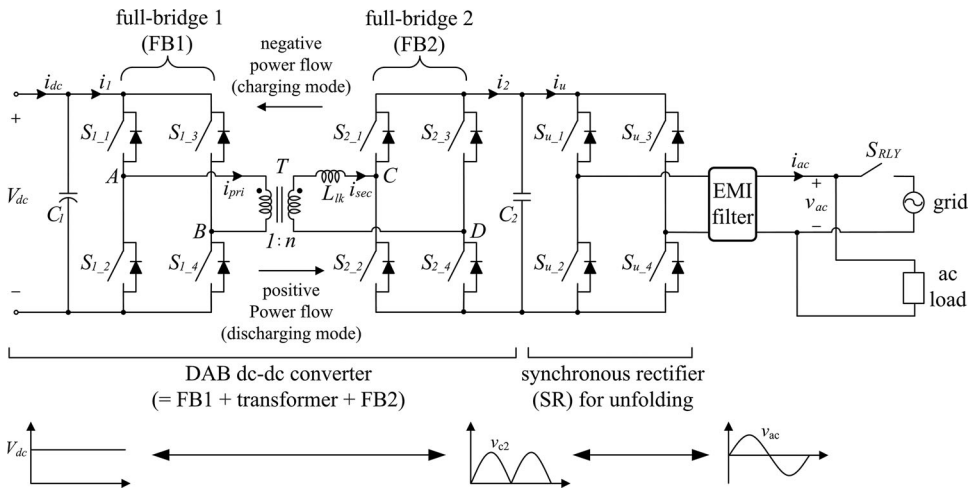

Fig. 2. Proposed bidirectional DAB inverter for the stand-alone generating system with single power-conversion stage.

inverter system in the conventional off-line UPS consists of an isolated step-up dc–dc converter, a inverter, and a dc-link capacitor with a high voltage that is higher than the peak voltage of the grid voltage such as the inverter system presented in [2] because the galvanic isolation is required to protect the system and prevent accidental current from reaching ground through a person's body. These inverter systems have unidirectional power flow, and requiring additional charger to charge the battery [3]–[8]. The single-stage or two-stage isolated power factor correction (PFC) ac–dc converters are used as the charger in UPSs. Therefore, the conventional stand-alone generating system for off-line UPSs has three or four power conversion stages as shown in Fig. 1(a).

In view of the power conversion, the conventional stand-alone generating systems for off-line UPSs can be expressed as shown in Fig. 1(a). The three or four power conversion stages, the hard switching in the inverter, and the use of more reactive elements lead to reduced efficiency, power density, and reliability and increase the cost of the overall system. To solve these problems, single-stage isolated bidirectional inverters have recently become a major research topic and have been proposed as an interface of the stand-alone power generating system [9]–[13]. Conventional stand-alone generating systems are simplified using single-stage isolated bidirectional inverters as shown in Fig. 1(b).

Dual-active-bridge (DAB) topologies are commonly used for single-stage isolated bidirectional inverters. DAB topologies offer bidirectional power flow, active power flow control, soft switching enabling a high-frequency operation, and isolation by a high-frequency transformer. The bidirectional power flow is gradually required because the traditional grid is evolving from a passive to a smart interactive service network, where energy systems play an active role in providing different types of support to the grid. The biggest advantage of DAB topologies is that the dc–ac energy conversions take place in a single power conversion stage without additional reactive elements, producing high-quality waveforms and complying by the regulations of the harmonic distortions of the grid [14].

The single-stage bidirectional DAB inverters are composed of the DAB dc–dc converter and synchronous rectifier (SR) as shown in Fig. 2. The DAB dc–dc converter converts a regulated dc input voltage to a rectified sinusoidal output voltage in phase with the grid voltage and back. Thus, without the additional grid-connected inverter, the output voltage of the DAB inverter synchronizes with the grid voltage and the grid current is controlled by a controller of the DAB dc–dc converter. The DAB inverter can be operated in two modes, namely, discharging mode and charging mode. For the charging mode, SR converts the ac voltage to the rectified sinusoidal voltage as the diode rectification. Although the switches in SR are operated at the grid frequency, since it changes only the direction of the ac voltage, which periodically reverses direction, to one direction and back, and therefore, the proposed stand-alone generating system for off-line UPSs is composed of only the bidirectional DAB inverter and has a single power conversion stage, as shown in Fig. 1(b).

In general, the basic modulation scheme of the bidirectional DAB converter is a phase shift modulation (PSM) that two full bridges (FBs) of the DAB converter are modulated with a 50% duty ratio and active power is controlled by a phase shift between two FBs. Although the PSM is simple, it has several drawbacks such as poor light-load efficiency, large reactive current flow, and limited soft switching range in presence of the wide variation in input–output voltages [15], [16]. Thus, this modulation scheme is unsuitable for bidirectional DAB inverters.

In recent years, various modulation schemes of DAB converters have been proposed and developed to overcome these drawbacks [17]–[24]. A trapezoidal modulation (TPZM) has three control parameters such as two duty ratios and a phase shift angle. Also, it has five modes in accordance with the relationship among three control parameters [21], [22]. A triangular modulation (TRM) is a special case of TPZM, where at one transition in every half cycle, two FBs are switched together, resulting in a triangular shape current waveform [22]. Since the power transfer capability of TRM is lower than PSM and TPZM, TRM is suitable for low power levels. Thus, the conventional hybrid

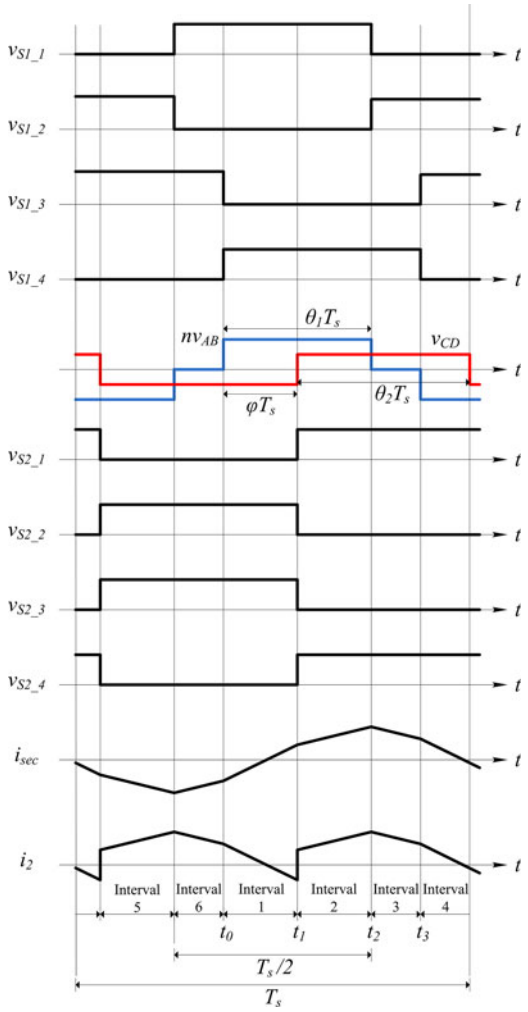

Fig. 3. Theoretical waveforms of the proposed DAB inverter.

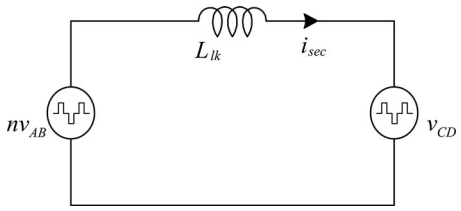

Fig. 4. Simplified electrical model of the proposed DAB inverter.

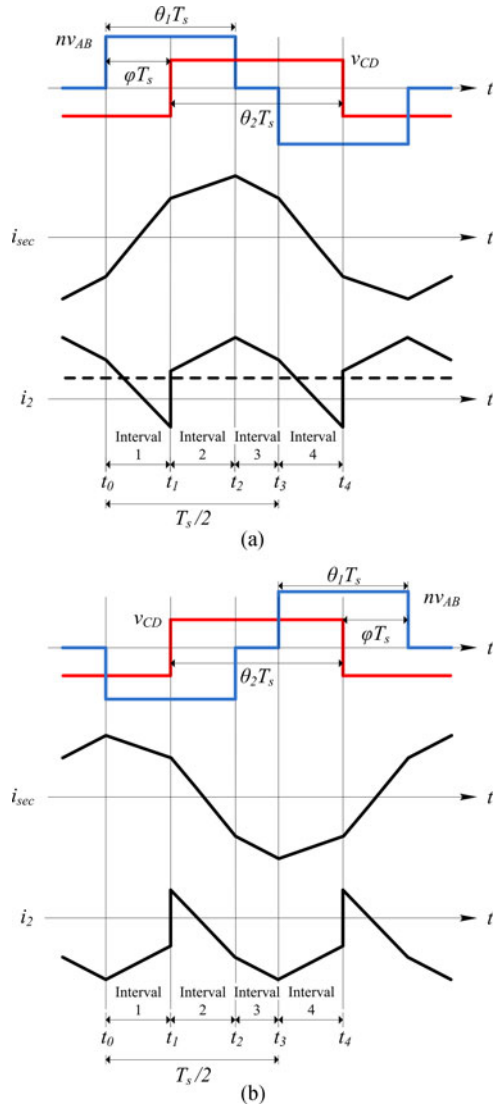

Fig. 5. Main waveforms of the proposed DAB inverter. (a) Waveforms in the positive flow. (b) Waveforms in the negative power flow.

modulation scheme combined with PSM, TRM, and TPZM is often used for bidirectional DAB inverters because they require a wide operating range [23], [24].

However, the control algorithm of the bidirectional DAB inverters using the conventional hybrid modulation is too complicated to implement a controller and is too difficult to optimize the control parameters because of the nonlinear relationship between the output current and the phase shift angle. Also, it is typically performed by lookup tables in which predetermined values for control parameters are stored and these values are the results of one particular system. Thus, the system using the conventional hybrid modulation is sensitive to changes of system parameters and the disturbance.

On the other hand, the control algorithm of a single H-bridge modulation (SHBM) which has two control parameters—a duty ratio and a phase shift angle—is easy to optimize and simple to implement, since the number of control parameters and modes according to the relation between a duty ratio and a phase shift angle is smaller than the conventional hybrid modulation. An SHBM has an inner mode and an outer mode in accordance with the relationship between two control parameters. A modulation scheme based on the inner mode has a linear power relationship, which leads to a simple closed-loop control for bidirectional DAB inverters [13]. However, since this modulation scheme results in an inductor current with a triangular waveform, the peak value of the inductor current is larger than that in other modulation schemes such as TPZM, PSM, and the outer mode of SHBM. This increases current stresses and core losses and decreases efficiency.

Stand-alone generating systems often have a low voltage battery as an energy storage element. The low-voltage dc power cannot directly support electrical appliances with the same power qualities of the grid in terms of frequency and

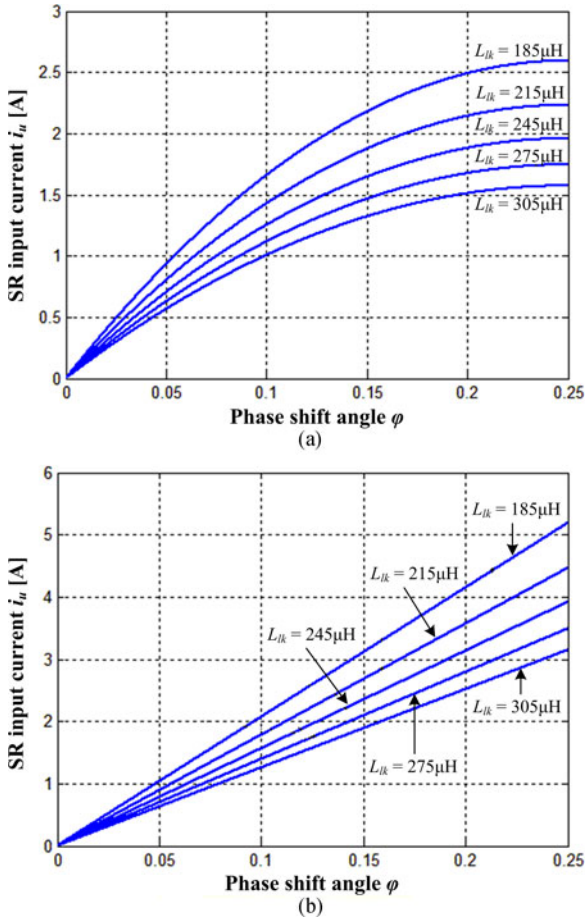

Fig. 6. Current control characteristic of the proposed DAB inverter. (a) SR input current i_u when only the phase shift control is used. (b) SR input current i_u when the novel hybrid modulation is used.

amplitude. Thus, to efficiently interface the low-voltage dc power to the electric utilities, a large voltage conversion ratio is an essential mechanism in both two-stage and single-stage stand-alone generating systems with low voltage battery. However, up to now, the abovementioned conventional modulation schemes have been optimized for single-stage or two-stage stand-alone generating systems with high-voltage battery. Since the DAB converter is a step-down converter, it must have a high secondary turn ratio to achieve the large voltage conversion ratio, which will result in high current stresses in the primary side of the converter. Therefore, the conventional modulation schemes in the stand-alone generating system with low voltage battery, especially the inner mode of SHBM, result in high current stresses and increase the transformer turn ratio.

In view of this, this paper proposes a high efficiency bidirectional DAB inverter using a novel hybrid modulation for a stand-alone power generating system with a low input voltage source. The proposed DAB inverter is composed of the DAB dc–dc converter and SR. The proposed DAB inverter provides single power conversion only. The hybrid modulation, a combination of a phase shift control and a variable frequency control, is used for the DAB dc–dc converter. The variable frequency control converts the nonlinear function of the phase shift angle into a linear function and controls the output power. The linear function in the phase shift control leads to a simple closed-loop control, low total harmonic distortion (THD), and unity power factor (PF). Also, the hybrid modulation provides a high-voltage conversion ratio without the increase of the transformer turn ratio. Analysis of the proposed DAB inverter is given and experimental results are obtained to show the performance and to verify the analysis.

II. Analysis of the Proposed DAB Inverter

A. Description of the Proposed Bidirectional DAB Inverter

Fig. 2 shows the proposed bidirectional DAB inverter for a stand-alone power generating system. The DAB dc–dc converter consists of two FBs and a transformer. The DAB dc–dc converter offers bidirectional power flow and active power flow control. Therefore, as shown in Fig. 2, the proposed DAB inverter comprises a DAB dc–dc converter with a high-voltage conversion ratio and SR for unfolding the rectified sinusoidal waveform. The primary FB (FB1) and the secondary FB (FB2) are connected to a dc source with low voltage $V_{\rm dc}$ and SR, respectively. The transformer has a high turn ratio of 1:n and the primary and secondary leakage inductance are lumped on the secondary as $L_{\rm lk}$. Since the transformer with high turn ratio has a relatively high leakage inductance $L_{\rm lk}$, either an external inductance or an integrated magnetic structure incorporating a series inductance is not required. The DAB dc–dc converter transforms the low dc voltage $V_{\rm dc}$ into the capacitor voltage v_{c2} that is pulsating twice the grid frequency f_L as shown in Fig. 2. The difference between the reflected output voltage nv_{AB} of FB1 and the output voltage $v_{\rm CD}$ of FB2 appears across the leakage inductance of a transformer and determines the direction and quantity of the power flow. When the grid voltage is normal, the switch $S_{\rm RLY}$ turns on to charge the internal storage battery and the ac loads are powered from the grid. When the grid voltage falls below or rises above a predetermined level, $S_{\rm RLY}$ turns off and the ac loads are powered by the proposed inverter for the stand-alone generating system. To analyze the proposed DAB inverter, the magnetizing inductance, winding resistances, and core losses of the transformer are all neglected and all switches are considered to be ideal except for their body diodes. During one period of the output voltage $v_{\rm ac}$, the state of SR changes twice according to the polarity of $v_{\rm ac}$. When the polarity of $v_{\rm ac}$ is positive, switches S_{u_1} and S_{u_4} are turned on and switches S_{u_2} and S_{u_3} are turned off. Conversely, when $v_{\rm ac}$ is negative, switches S_{u_1} and S_{u_4} are turned off and switches S_{u_2} and S_{u_3} are turned on. Consequently, the voltage v_{c2} across the capacitor C_2 is unfolded into $v_{\rm ac}$. Since all switches in SR operate at the grid frequency f_L, the switching losses of those switches are very small.

B. Novel Hybrid Modulation for the Proposed Bidirectional DAB Inverter

The novel hybrid modulation combines a phase shift control and a variable frequency control. Fig. 3 shows the theoretical waveforms of the proposed DAB inverter using the hybrid

modulation scheme in the positive power flow. All switches are modulated with a 50% duty ratio and a top switch is complemented with a bottom switch with a short dead time in each leg. The phase shift angle θ_1 is the phase difference between a leg *A* and a leg *B* and the phase shift angle θ_2 is the phase difference between a leg *C* and a leg *D*. The output voltage v_{AB} of FB1 and the output voltage $v_{\rm CD}$ of FB2 are generated by θ_1 and θ_2, respectively. Since the proposed hybrid modulation bases on the outer mode of SHBM, θ_2 is a half of a switching period T_s and the phase shift angle φ that is the phase difference between $v_{\rm AB}$ and $v_{\rm CD}$ is smaller than θ_1 as shown in Fig. 3. In this hybrid modulation, φ is always a half of θ_1. Thus, the active power can be controlled by one of θ_1 and φ.

On the assumption of ideal components and by referring the model to the secondary side of the transformer, Figs. 4 and 5 show the simplified electrical model and main waveforms of the proposed DAB inverter, respectively. The theoretical waveforms of the secondary current $i_{\rm sec}$ flowing through $L_{\rm lk}$ of the transformer, the voltage source nv_{AB} connected to left side of $L_{\rm lk}$, and the voltage source $v_{\rm CD}$ connected to right side of $L_{\rm lk}$ in Fig. 4 are shown in Fig. 5.

In the positive power flow, the steady-state operation of the proposed DAB inverter includes six intervals in one switching period. The waveforms of nv_{AB} and $v_{\rm CD}$ are the rectangular pulse wave whose pulse width is modulated with θ_1 and θ_2, respectively. Also, they pulsate from $nV_{\rm dc}$ to $-nV_{\rm dc}$ and from $|v_{\rm ac}|$ to $|-v_{\rm ac}|$, respectively. As shown in Fig. 5(a), since $|v_{\rm ac}|$is approximately constant during one switching period T_s, $i_{\rm sec}$ in each interval increases or decreases linearly with the following slopes:

$$\frac{di_{\rm sec}}{dt} = \begin{cases} \dfrac{nV_{\rm dc}+|v_{\rm ac}|}{L_{\rm lk}}, & \text{for interval 1} \\ \dfrac{nV_{\rm dc}-|v_{\rm ac}|}{L_{\rm lk}}, & \text{for interval 2} \\ \dfrac{-|v_{\rm ac}|}{L_{\rm lk}}, & \text{for interval 3} \end{cases} \tag{1}$$

The waveforms of nv_{AB}, $v_{\rm CD}$, and $i_{\rm sec}$ in the intervals 1–3 and the intervals 4–6 are symmetric with respect to the *t*-axis in Fig. 5. Thus, $i_{\rm sec}(t_4)$ is equal to $-i_{\rm sec}(t_1)$. From this relationship and (1), $i_{\rm sec}(t_1)$ can be obtained as

$$i_{\rm sec}(t_1) = \frac{0.5|v_{\rm ac}| + nV_{\rm dc}(2\varphi-\theta_1)}{L_{lk}} T_s. \tag{2}$$

The waveforms of the output current i_2 of FB2 in the intervals 1–3 are equal to those waveforms in the intervals 4–6 as shown in Fig. 3. Also, since the ripple of the SR input current i_u is small enough to neglect the effect, the average current $i_{2,\rm avg}$ of i_2 is equal to i_u and the rectified output current $|i_{\rm ac}|$. Thus, i_u can be written as follows:

$$i_u = i_{2,\rm avg} = \frac{2}{T_s}\int_{t_1}^{t_4} i_2(t)dt. \tag{3}$$

From (1)–(3), i_u is obtained as follows:

$$i_u = \frac{nV_{\rm dc}T_s}{L_{lk}}\left(-\theta_1^2 - 2\varphi^2 + 2\varphi\theta_1 + 0.5\theta_1\right). \tag{4}$$

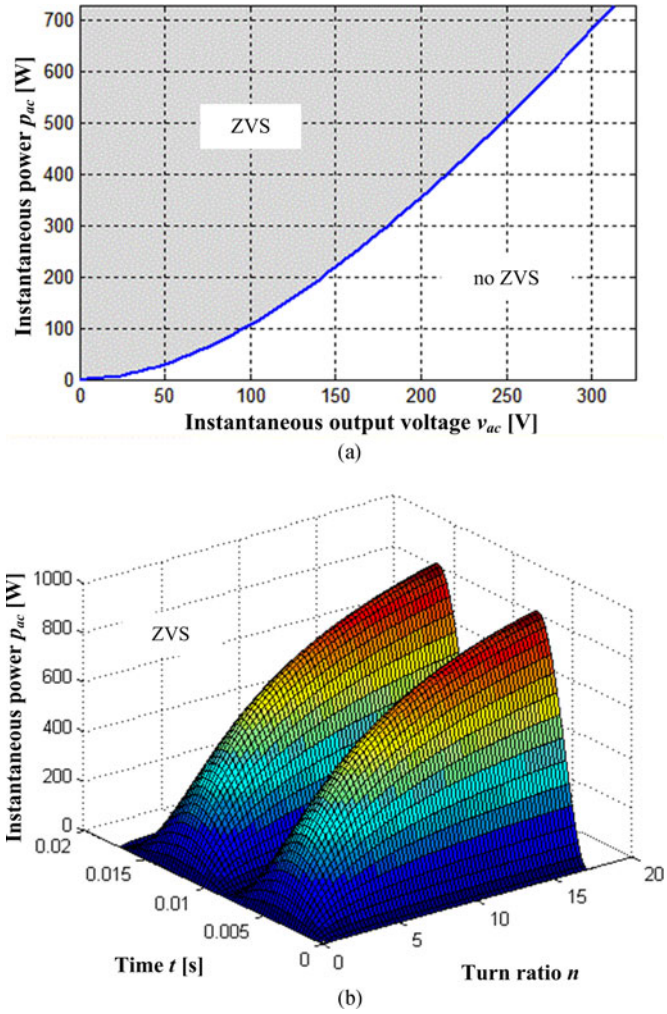

Fig. 7. ZVS region of switches S_{1_3} and S_{1_4}. (a) The critical value of the function $p_{\rm ac}(v_{\rm ac})$ to satisfy the ZVS condition. (b) The critical value of the function $p_{\rm ac}(t,n)$ to satisfy the ZVS condition.

In the proposed hybrid modulation, θ_1 is twice as large as the phase shift angle φ. Thus, i_u is rewritten as follows:

$$i_u = \frac{nV_{\rm dc}T_s}{L_{lk}}\left(\varphi - 2\varphi^2\right). \tag{5}$$

Fig. 6 shows the current control characteristic of the proposed DAB inverter at $V_{\rm dc} = 48$ V, $n = 8$, $L_{\rm lk} = 185\,\mu$H, and $T_s = 10$ μs. Fig. 6(a) shows the SR input current i_u when only the phase shift control is used. All modulation schemes for DAB converters except for the inner mode of SHBM have a nonlinear function of the control variable. The proposed DAB inverter also has a nonlinear function. This can be verified by Fig. 6(a) and (5). To achieve good controllability of the proposed DAB inverter, the nonlinear relationship between i_u and φ needs to be transformed into a linear relationship. The variable frequency control in the hybrid modulation changes the relationship from nonlinear to linear by using the switching frequency function $f_s(\varphi)$ as follows:

$$f_s(\phi) = f_{s\_\rm var}\left(1 - 2\varphi\right) \tag{6}$$

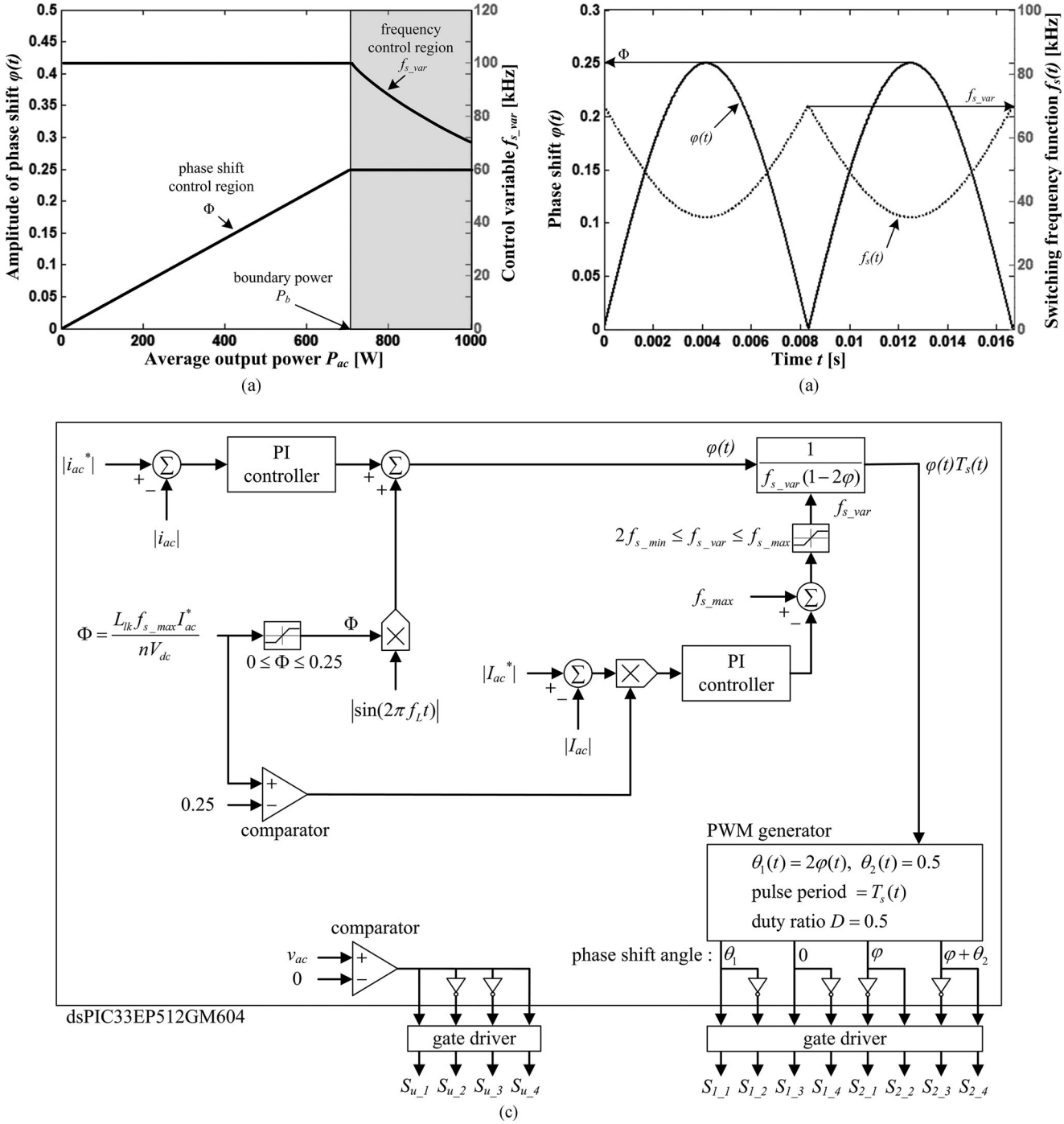

Fig. 8. Control variables during the grid period T_L in positive power flow. (a) Control variables Φ and f_{s_var} for the output power control. (b) Control variables $\varphi(t)$ and $f_s(t)$ for the output current i_{ac} with a sinusoidal waveform in phase with v_{ac}. (c) Control block diagram.

where f_{s_var} is the control variable in the variable frequency control. Therefore, (5) can be expressed as follows:

$$i_u = \frac{nV_{\mathrm{dc}}}{L_{\mathrm{lk}} f_s(\varphi)} \left(\varphi - 2\varphi^2\right) = \frac{nV_{\mathrm{dc}}}{L_{\mathrm{lk}} f_{s\_\mathrm{var}}} \varphi. \tag{7}$$

Fig. 6(b) shows the SR input current i_u when the novel hybrid modulation is used. From (7) and Fig. 6(b), it can be verified that the proposed DAB inverter with the novel hybrid modulation has the linear relationship between i_u and φ.

To achieve the high efficiency, it is important to reduce the switching losses of switches. Since the proposed DAB inverter achieves the zero-voltage switching (ZVS) turn on in the heavy load condition, switching losses are small. However, the hard-switching region exists in the light load condition. For the ZVS turn on of switches S_{1_1} and S_{1_2}, i_{sec} at time t_2 should be positive. From (1) and (2), $i_{\mathrm{sec}}(t_2)$ can be derived as

$$i_{\mathrm{sec}}(t_2) = \frac{T_s}{L_{lk}} \left[\left(nV_{\mathrm{dc}} - |v_{\mathrm{ac}}|\right) \varphi + \frac{|v_{\mathrm{ac}}|}{4} \right] \ge 0. \tag{8}$$

TABLE I
PARAMETERS AND COMPONENTS OF THE PROTOTYPE

Parameters	Symbols	Value
Input voltage	$V_{\rm dc}$	42–54V
Switching frequency	f_s	35–100 kHz
Grid voltage	$v_{\rm ac}$	220 V
Grid frequency	f_L	60 Hz
Input capacitor	C_1	3300 μF
DC-link capacitor	C_2	1 μF
Secondary leakage inductance	L_{lk}	185 μH
Primary winding turns	N_p	4 turns
Secondary winding turns	N_s	32 turns
Components	Symbols	Part number
Switches of FB1	$S_{1_1}, S_{1_2}, S_{1_3}, S_{1_4}$	IPPO30N10N
Switches of FB2	$S_{2_1}, S_{2_2}, S_{2_3}, S_{2_4}$	IRFPS43N50K
Switches of SR	$S_{u\_1}, S_{u\_2}, S_{u\_3}, S_{u\_4}$	IRFPS43N50K
Transformer core	T	PQ5050

Since $nV_{\rm dc}$ should be always larger than $|v_{\rm ac}|$, $i_{\rm sec}(t_2)$ is larger than zero in the overall load condition. It means that the switches S_{1_1} and S_{1_2} achieve the ZVS turn on in the overall load condition. All switches in FB2 achieve the ZVS turn on when $i_{\rm sec}$ at time t_1 is positive. From the fact that θ_1 is twice as large as the phase shift angle φ, (2) can be expressed as follows:

$$i_{\rm sec}(t_1) = \frac{|v_{\rm ac}|}{4L_{\rm lk}} \geq 0. \tag{9}$$

Since $i_{\rm sec}(t_1)$ is always larger than zero, the switches in FB2 achieve the ZVS turn on in the overall load condition. To achieve the ZVS turn on of switches S_{1_3} and S_{1_4}, $i_{\rm sec}$ at the time t_3 should be positive. From (1), (8), and (9), $i_{\rm sec}(t_3)$ is obtained as follows:

$$i_{\rm sec}(t_3) = nV_{\rm dc}\varphi + |v_{\rm ac}|\varphi - \frac{|v_{\rm ac}|}{4} \geq 0. \tag{10}$$

From (10), for the ZVS turn on of these switches, the following condition must be satisfied:

$$\varphi \geq \frac{|v_{\rm ac}|}{4\left(nV_{\rm dc} + |v_{\rm ac}|\right)}. \tag{11}$$

When the output voltage $v_{\rm ac}$ is equal to the grid voltage, $v_{\rm ac}$ is

$$v_{\rm ac}(t) = V_{\rm ac}\sin(2\pi f_L t) \tag{12}$$

where $V_{\rm ac}$ is the amplitude of the grid voltage. From (7), (11), and (12), the load condition for the ZVS turn on of switches S_{1_3} and S_{1_4} can be obtained as follows:

$$p_{\rm ac}(t) = |v_{\rm ac}||i_{\rm ac}| \geq \frac{nV_{\rm dc}|v_{\rm ac}|^2 T_s}{4L_{lk}\left(nV_{\rm dc} + |v_{\rm ac}|\right)}. \tag{13}$$

Fig. 7 shows the ZVS region of switches S_{1_3} and S_{1_4} at $V_{\rm dc} = 48$ V, $n = 8$, $L_{\rm lk} = 185$ μH, $V_{\rm ac} = 311$ V, and $T_s = 10$ μs. The critical instantaneous output power $p_{\rm ac}(v_{\rm ac})$ value to satisfy the ZVS turn on condition of those switches according to the variation of the instantaneous output voltage $v_{\rm ac}$ can be seen from (13) and Fig. 7(a). Fig. 7(b) shows the three-dimensional (3-D) plot about the critical value of the instantaneous output power function $p_{\rm ac}(t, n)$ of variables time t and turn ratio n to satisfy the ZVS condition of those switches. As the turn ratio n increases, the critical output power value $p_{\rm ac}(t, n)$ increases in Fig. 7(b). It means that the smaller turn ratio n is good to increase the ZVS region. However, since the stand-alone generating systems with low dc voltage source require a high-voltage conversion ratio, these systems have a transformer with a relatively high turn ratio n. Also, the increase of n leads to the increase of the leakage inductance of the transformer. It can be seen that the increase of the leakage inductance reduces the output power from (7). This problem can be solved by using the variable frequency control in the hybrid modulation. The role of the variable frequency control is not only the conversion of nonlinear relationship between i_u and φ into linear relationship but also the output power control. When unity power factor is achieved, the output current $i_{\rm ac}$ is a sinusoidal waveform in phase with $v_{\rm ac}$ as

$$i_{\rm ac}(t) = I_{\rm ac}\sin(2\pi f_L t) \tag{14}$$

where $I_{\rm ac}$ is the amplitude of $i_{\rm ac}$. From (14), the current i_u is

$$i_u(t) = |i_{\rm ac}(t)| = |I_{\rm ac}\sin(2\pi f_L t)|. \tag{15}$$

Since i_u is directly proportional to φ when using the hybrid modulation, the phase shift angle φ should be a rectified sine wave in phase with $i_{\rm ac}$ as a following function $\varphi(t)$ to achieve unity power factor:

$$\varphi(t) = |\Phi\sin(2\pi f_L t)| \tag{16}$$

where Φ is the amplitude of the phase shift angle $\varphi(t)$. From (7) and (16), (15) can be rewritten as follows:

$$i_u(t) = I_{\rm ac}|\sin(2\pi f_L t)| = \frac{nV_{\rm dc}\Phi}{L_{lk} f_{s\_\rm var}}|\sin(2\pi f_L t)|. \tag{17}$$

From (17), the amplitude of $\varphi(t)$ can be obtained as follows:

$$\Phi = \frac{I_{\rm ac} L_{lk} f_{s\_\rm var}}{nV_{\rm dc}}. \tag{18}$$

When unity power factor is achieved, the output power $p_{\rm ac}(t)$ is

$$\begin{aligned} p_{\rm ac}(t) &= V_{\rm ac} I_{\rm ac}\sin(2\pi f_L t)^2 = 2P_{\rm ac}\sin(2\pi f_L t)^2 \\ &= \frac{nV_{\rm dc}V_{\rm ac}\Phi}{L_{lk} f_{s\_\rm var}}\sin(2\pi f_L t)^2 \end{aligned} \tag{19}$$

where $P_{\rm ac}$ is the average output power of the proposed DAB inverter and is expressed as

$$P_{\rm ac} = \frac{nV_{\rm dc}V_{\rm ac}\Phi}{2L_{lk} f_{s\_\rm var}}. \tag{20}$$

From (20), the decrease of $f_{s\_\rm var}$ increases the output power $P_{\rm ac}$ without the increase of the turn ratio n.

Fig. 8 shows the control variables during the grid period T_L in positive power flow at $V_{\rm dc} = 42$ V, $n = 8$, $L_{\rm lk} = 185$ μH, and $V_{\rm ac} = 311$ V. All phase shift angles θ_1, θ_2, and φ are normalized. The minimum and maximum angles are 0° and 360°, respectively. Since the proposed hybrid modulation bases on the outer mode of SHBM, θ_2 is always 0.5 and θ_1 ranges from 0 to 0.5. The phase shift angle φ in the discharging and charging modes is defined as shown in Fig. 5(a) and (b), respectively.

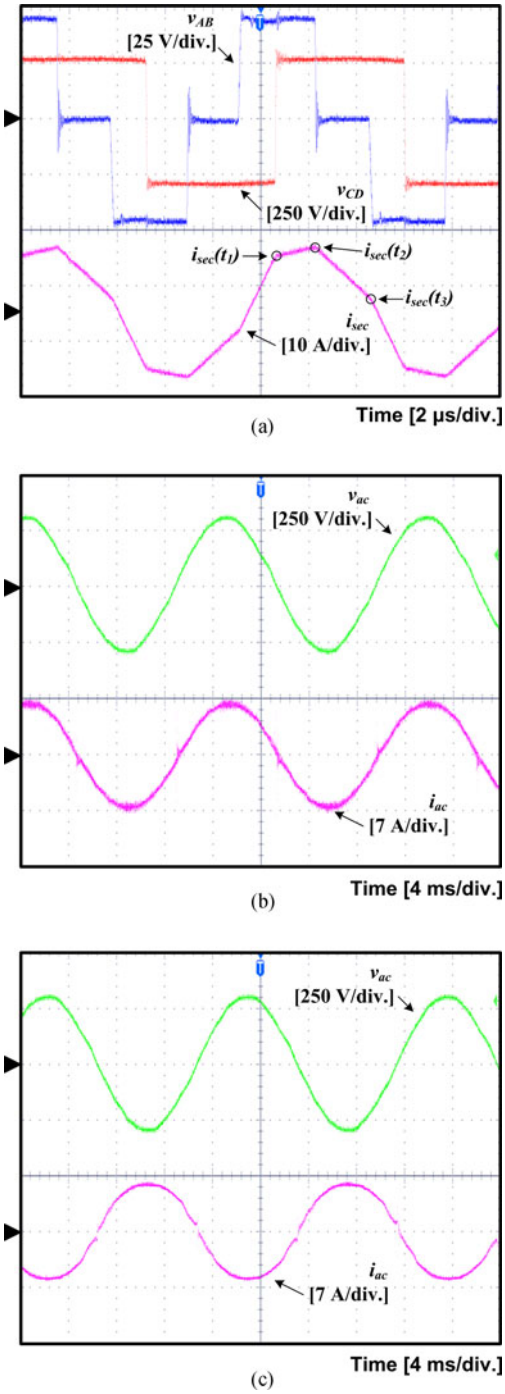

Fig. 9. Experimental waveforms of the prototype. (a) The output voltage v_{AB} fo FB1, the output voltage v_{CD} of FB2, and the secondary current $i_{\rm sec}$ in positive power flow. (b) $v_{\rm ac}$ and $i_{\rm ac}$ in positive power flow. (c) $v_{\rm ac}$ and $i_{\rm ac}$ in negative power flow.

Also, φ is always a half of θ_1 in the proposed hybrid modulation. Therefore, φ ranges from 0 to 0.25. From (16), the range of Φ can be obtained as follows:

$$0 \le \Phi \le 0.25. \tag{21}$$

Fig. 8(a) is divided into two regions which are the phase shift control region and the frequency control region. The boundary power P_b is the average output power when Φ reaches 0.25. When the output power $P_{\rm ac}$ is under P_b, the proposed inverter operates in the phase shift control region and $P_{\rm ac}$ is controlled by adjusting Φ of $\varphi(t)$. When $P_{\rm ac}$ is above P_b, the proposed inverter operates in the frequency control region and Φ is constant at 0.25. In this region, $P_{\rm ac}$ can be changed by adjusting the control variable $f_{s\_\rm var}$. Fig. 8(b) shows the control variables $\varphi(t)$ and $f_s(t)$ for $i_{\rm ac}$ with a sinusoidal waveform in phase with $v_{\rm ac}$ at the average output power $P_{\rm ac}$ of 1 kW. Fig. 8(c) shows the control block diagram of the proposed inverter. Although the phase shift control region and the frequency control region are divided on the basis of the boundary power P_b, since P_b is the average output power when Φ reaches 0.25, they are practically divided on Φ as shown in Fig. 8(c). When Φ is over 0.25, Φ is fixed by the limiter at 0.25 and $f_{s\_\rm var}$ is determined by a proportional–integral (PI) controller. The range of the switching frequency $f_s(t)$ is

$$f_{s\_\min} \le f_s(t) \le f_{s\_\max} \tag{22}$$

where $f_{s\_\min}$ and $f_{s\_\max}$ are the minimum and the maximum switching frequency, respectively. From (6), (16), and (22), the range of $f_{s\_\rm var}$ can be obtained as follows:

$$2f_{s\_\min} \le f_{s\_\rm var} \le f_{s\_\max}. \tag{23}$$

When Φ is under 0.25, $f_{s\_\rm var}$ is fixed by the comparator at $f_{s\_\max}$ and $p_{\rm ac}$ is controlled by $\varphi(t)$.

Fig. 5(b) shows the main waveforms of the proposed DAB inverter in the negative power flow. The instantaneous power is transferred from the secondary to the primary side of the transformer which demands a different sign of nv_{AB} and $i_{\rm sec}$. In the negative power flow, the analytical expression of $i_{\rm sec}$, i_u, and $p_{\rm ac}$ can be obtained the same way as in positive power flow considering six intervals from Fig. 5(b).

III. Experimental Results

An experimental prototype was implemented to show the performance and to verify the theoretical analysis of the proposed bidirectional DAB inverter and the hybrid modulation. Also, it was tested under the condition that the inverter was connected to the grid. The prototype is designed for the rated output power $P_{\rm ac} = 1$ kW and the detailed information of the design of the prototype is described in Table I. The switch $S_{\rm RLY}$ for grid connection is implemented by a relay HR-CR3A11DC12KH. For testing of the prototype system, four lead-acid batteries with 12V/100 Ah which are connected in series are used as low voltage dc source at the input of the DAB inverter. The electromagnetic interference filter is essential for eliminating high-frequency harmonic currents from the ac source current and the electromagnetic interference. The control system is implemented in software using a single-chip microcontroller, Microchip dsPIC33EP512GM604. It is responsible for generating the pulsewidth-modulated (PWM) gate drive signals, sensing in the current and voltage measurement peripherals (12 bit A/D converters), overcurrent and overvoltage protection, and dead-time compensation.

Fig. 9 shows the experimental waveforms of the proposed DAB inverter. Fig. 9(a) shows the output voltage $v_{\rm AB}$ of FB1, the output voltage $v_{\rm CD}$ of FB2, and the secondary current $i_{\rm sec}$ at

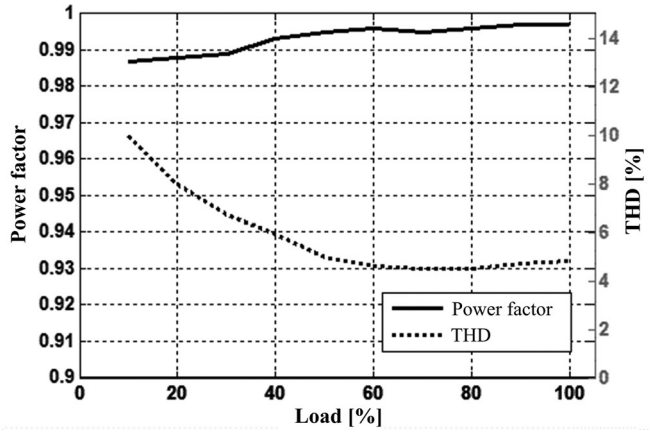

Fig. 10. Measured PF and THD of the output current $i_{\rm ac}$.

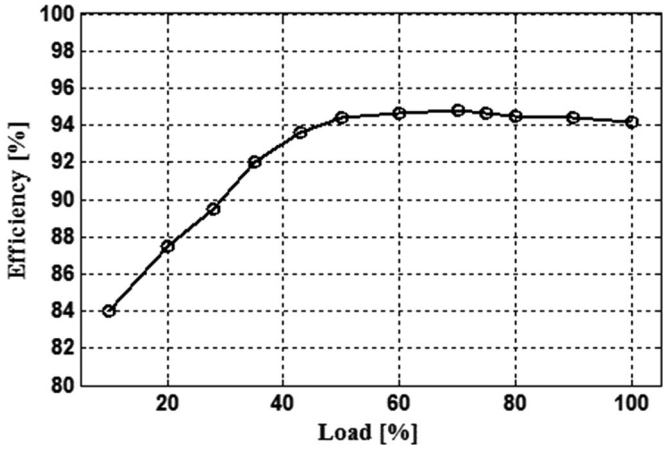

Fig. 11. Measured power efficiency under entire load conditions.

one point in the grid period. As mentioned above, since $i_{\rm sec}$ has a positive value at all points of t_1, t_2, and t_3, all switches of FB1 and FB2 achieve the ZVS turn on. Fig. 9(b) and (c) show the experimental waveforms of the output voltage $v_{\rm ac}$ and current $i_{\rm ac}$ in the positive power flow and the negative power flow, respectively. Since the output current $i_{\rm ac}$ in Fig. 9(b) and (c) is a sinusoidal waveform in phase with $v_{\rm ac}$ according to power flow, the proposed DAB inverter achieves the unity PF and low THD in both positive and negative power flow. However, THD of the output current $i_{\rm ac}$ in positive power flow is lower than that in negative power flow. The proposed DAB inverter has a dead time in their gate signals. The dead time has an impact in the behavior of the system compared to the ideal one without the dead time. The effect of the dead time in THD is clearly not symmetrical. This is due to the fact that the dead time is equivalent to an added phase, but this phase has always the same direction. The effect is considerable at low angles, and decreases as the phase increases. The proposed DAB inverter is optimized by dead time compensation for only the dc–ac power conversion. Therefore, $i_{\rm ac}$ in negative power flow has a higher THD than in positive power flow.

Fig. 10 shows the measured PF and THD of the output current $i_{\rm ac}$ in the whole power. The prototype was successfully tested in the full power range up until an output power of 1 kW. It achieves the high PF close to unity and low THD in the whole power. Fig. 11 shows the measured power efficiency of the proposed DAB inverter under all load conditions. Although the proposed DAB inverter has low dc voltage source, it achieves the high efficiency in heavy load conditions. However, as the output power decreases, the no ZVS turn-on region and the switching frequency of the DAB converter increase, which cause the switching loss increase significantly. The maximum efficiency of the proposed DAB inverter is 94.8% and the efficiency at rated power is 94.2%. The efficiency is measured by the digital power meter Yokogawa WT130.

IV. Conclusion

This paper has proposed a high-efficiency bidirectional DAB inverter using a novel hybrid modulation for a stand-alone power generating system with low input voltage. Also, analysis and experimental results for the proposed DAB inverter using the novel hybrid modulation have been presented. The proposed DAB inverter consists of a DAB dc–dc converter composed of two FBs and a transformer and SR for unfolding the rectified sinusoidal waveform. The low dc voltage is converted into the rectified sinusoidal waveform through the DAB dc–dc converter and the rectified sinusoidal waveform is unfolded into the grid voltage with the sine wave. Thus, the proposed DAB inverter has only single power conversion stage. The novel hybrid modulation used in the proposed DAB inverter is composed of a phase shift control and a variable frequency control. The variable frequency control makes the nonlinear relation between i_u and φ into a linear relationship. Also, it provides the high-voltage conversion ratio without the increase of the transformer turn ratio. The linear relationship results in a simple closed-loop control, a low THD, and a high PF close to unity. The 1 kW prototype has high efficiency of 94.2% by the ZVS turn on of the switches of FB1 and FB2. The proposed DAB inverter using the novel hybrid modulation is a promising solution for high power applications, where efficiency, cost, and power density are important and isolation is required.

References

[1] M. H. Ryu, D. G. Jung, and J. W. Baek, "An optimized design of bi-directional dual active bridge converter for low voltage charger," in *Proc. IEEE 16th Int. Power Electron. Motion Control Conf.*, Sep. 2014, pp. 177–183.

[2] J. M. Kwon, E. H. Kim, B. H. Kwon, and K. H. Nam, "High-efficiency fuel cell power conditioning system with input current ripple reduction," *IEEE Trans. Ind. Electron.*, vol. 59, no. 3, pp. 826–834, Mar. 2009.

[3] S. K. Mazumder, R. K. Burra, and K. Acharya, "A ripple-mitigating and energy-efficient fuel cell power-conditioning system," *IEEE Trans. Power Electron.*, vol. 22, no. 4, pp. 1437–1452, Jul. 2007.

[4] F. Blaabjerg, Z. Chen, and S. B. Kjaer, "Power electronics as efficient interface in dispersed power generation systems," *IEEE Trans. Power Electron.*, vol. 19, no. 5, pp. 1184–1194, Sep. 2004.

[5] W. J. Cha, Y. W. Cho, J. M. Kwon, and B. H. Kwon, "Highly Efficient Microinverter With Soft-Switching Step-Up Converter and Single-Switch-Modulation Inverter," *IEEE Trans. Ind. Electron.*, vol. 62, no. 6, pp. 3516–3523, Jun. 2015.

[6] E. Serban and H. Serban, "A control strategy for a distributed power generation microgrid application with voltage and current controlled source

converter," *IEEE Trans. Power Electron.*, vol. 25, no. 12, pp. 2981–2992, Dec. 2010.
[7] Z. Ye, P. K. Jani, and P. C. Sen, "A Full-Bridge Resonant Inverter With Modified Phase-Shift Modulation for High-Frequency AC Power Distribution Systems," *IEEE Trans. Ind. Electron.*, vol. 54, no. 5, pp. 2831–2845, Oct. 2007.
[8] J. Kan, S. Xie, Y. Wu, Y. Tang, Z. Yao, and R. Chen, "Single-Stage and Boost-Voltage Grid-Connected Inverter for Fuel-Cell Generation System," *IEEE Trans. Ind. Electron.*, vol. 62, no. 9, pp. 5480–5490, Sep. 2015.
[9] B. Singh, B. N. Singh, A. Chandra, K. Al-Haddad, A. Pandey, and D. P. Kothari, "A review of single-phase improved power quality AC–DC converters," *IEEE Trans. Ind. Electron.*, vol. 50, no. 5, pp. 962–981, Oct. 2003.
[10] F. Jauch and J. Biela, "Single-phase single-stage bidirectional isolated ZVS ac–dc converter with PFC," in *Proc. IEEE 15th Int. Power Electron. Motion Control Conf.*, Sep. 2012, pp. 1–8, Paper LS5d.1.
[11] J. Everts, F. Krismer, J. Van den Keybus, J. Driesen, and J. W. Kolar, "Comparative evaluation of soft-switching, bidirectional, isolated AC/DC converter topologies," in *Proc. IEEE 27th Ann. Appl. Power Electron. Conf. Expo.*, Feb. 2012, pp. 1067–1074.
[12] J. Everts, F. Krismer, J. Van den Keybus, J. Driesen, and J. W. Kolar, "Optimal ZVS modulation of single-phase single-stage bidirectional DAB AC-DC converters," *IEEE Trans. Power Electron.*, vol. 29, no. 8, pp. 3954–3970, Aug. 2014.
[13] N. D. Weise, G. Castelino, K. Basu, and N. Mohan, "A single-stage dual-active-bridge-based soft switched ac–dc converter with open-loop power factor correction and other advanced features," *IEEE Trans. Power Electron.*, vol. 29, no. 8, pp. 4007–4016, Aug. 2014.
[14] M. H. Kheraluwala and R. W. De Doncker, "Single phase unity power factor control for dual active bridge converter," in *Proc. IEEE Ind. Appl. Soc. Annu. Meeting*, Oct. 1993, vol. 2, pp. 909–916.
[15] R. De Doncker, D. Divan, and M. Kheraluwala, "A three-phase soft-switched high-power-density dc/dc converter for high-power applications," *IEEE Trans. Ind. Appl.*, vol. 27, no. 1, pp. 63–73, Jan./Feb. 1991.
[16] M. Kheraluwala, R. Gascoigne, D. Divan, and E. Baumann, "Performance characterization of a high-power dual active bridge dc-to-dc converter," *IEEE Trans. Ind. Appl.*, vol. 28, no. 6, pp. 1294–1301, Nov./Dec. 1992.
[17] H. Bai and C. Mi, "Eliminate reactive power and increase system efficiency of isolated bidirectional dual-active-bridge dc–dc converters using novel dual-phase-shift control," *IEEE Trans. Power Electron.*, vol. 23, no. 6, pp. 2905–2914, Nov. 2008.
[18] R. J. Wai, C. Y. Lin, C. Y. Lin, R. Y. Duan, and Y. R. Chang, "High-efficiency power conversion system for kilowatt-level stand-alone generation unit with low input voltage," *IEEE Trans. Ind. Electron.*, vol. 55, no. 10, pp. 3702–3714, Oct. 2008.
[19] B. Zhao, Q. Song, and W. Liu, "Power characterization of isolated bidirectional dual-active-bridge dc–dc converter with dual-phase-shift control," *IEEE Trans. Power Electron.*, vol. 27, no. 9, pp. 4172–4174, Sep. 2012.
[20] F. Krismer and J. W. Kolar, "Closed form solution for minimum conduction loss modulation of DAB converters," *Trans. Power Electron.*, vol. 27, no. 1, pp. 174–188, Jan. 2012.
[21] A. K. Jain and R. Ayyanar, "PWM control of dual active bridge: Comprehensive analysis and experimental verification," *IEEE Trans. Power Electron.*, vol. 26, no. 4, pp. 1215–1227, Apr. 2011.
[22] H. Zhou and A. M. Khambadkone, "Hybird modulation for dual-active-bridge bidirectional converter with extended power range for ultracapacitor application," *IEEE Trans. Ind. Appl.*, vol. 45, no. 4, pp. 1434–1442, Jul./Aug. 2009.
[23] F. Krismer, S. Round, and J. Kolar, "Performance optimization of a high current dual active bridge with a wide operating voltage range," in *Proc. IEEE Power Electron. Spec. Conf.*, 2006, pp. 1–7.
[24] Y. Wang, S. W. H. De Haan, and J. Ferreira, "Optimal operating ranges of three modulation methods in dual active bridge converters," in *Proc. IEEE Power Electron. Motion Contr. Conf.*, 2009, pp. 1397–1401.

Yong-Won Cho was born in Daegu, Korea, in 1983. He received the B.S. degree in electrical engineering from Kyungpook National University, Daegu, Korea, in 2009. He is currently working toward the Ph.D. degree in electronic and electrical engineering at the Pohang university of Science and Technology (POSTECH), Pohang, Korea.

His current research interests include switched-mode power supplies and dc–dc converters.

Woo-Jun Cha was born in Inchon, Korea, in 1979. He received the M.S. degree in electronic systems engineering from Hanyang University, Ansan, Korea, in 2013. He is currently working toward the Ph.D. degree in electronic and electrical engineering at the Pohang university of Science and Technology (POSTECH), Pohang, Korea.

His current research interests include the photovoltaic system, switched-mode power supply, and advanced LED lighting solutions.

Jung-Min Kwon (S'08–M'09) was born in Ulsan, Korea, in 1981. He received the B.S. degree in electrical and electronic engineering from Yonsei University, Seoul, Korea, in 2004, and the Ph.D. degree in electronic and electrical engineering from Pohang University of Science and Technology (POSTECH), Pohang, Korea, in 2009.

From 2009 to 2011, he was with the Samsung Advanced Institute of Technology, Yongin, Korea. Since 2011, he has been with the Department of Electrical Engineering, Hanbat National University, Daejeon, Korea, where he is currently a Professor. His current research interests include direct methanol fuel cell, renewable energy system, and distributed generation.

Bong-Hwan Kwon (M'91) was born in Pohang, Korea, in 1958. He received the B.S. degree from the Kyungpook National University, Deagu, Korea, in 1982, and the M.S. and Ph.D. degrees in electrical engineering from the Korea Advanced Institute of Science and Technology, Seoul, Korea, in 1984 and 1987, respectively.

Since 1987, he has been with the Department of Electronic and Electrical Engineering, Pohang University of Science and Technology (POSTECH), Pohang, Korea, where he is currently a Professor. His current research interests include converters for renewable energy, high-frequency converters, and switched-mode power supplies.